

Time-resolved interaction proteomics of the GIGANTEA protein under diurnal cycles in *Arabidopsis*

Johanna Krahmer^{1,2}, Greg S. Goralogia³, Akane Kubota^{3,4}, Argyris Zardilis¹, Richard S. Johnson⁵, Young Hun Song^{3,6}, Michael J. MacCoss⁵, Thierry Le Bihan¹, Karen J. Halliday², Takato Imaizumi³ and Andrew J. Millar¹ 

1 SynthSys and School of Biological Sciences, University of Edinburgh, UK

2 Institute of Molecular Plant Sciences, University of Edinburgh, UK

3 Department of Biology, University of Washington, Seattle, WA, USA

4 Graduate School of Biological Sciences, Nara Institute of Science and Technology, Ikoma, Nara, Japan

5 Department of Genome Sciences, University of Washington, Seattle, WA, USA

6 Department of Life Sciences, Ajou University, Suwon, Korea

Correspondence

A. J. Millar, SynthSys, C.H. Waddington Building, University of Edinburgh, Max Born Crescent, Edinburgh EH9 3BF, Scotland, UK

Tel: +44 (0)131 651 3325

E-mail: Andrew.Millar@ed.ac.uk

and

T. Imaizumi, Department of Biology, University of Washington, 24 Kincaid Hall, Box 351800, Seattle, WA 98195-1800, USA

Tel: +1 206 543 8709

E-mail: takato@uw.edu

(Received 20 August 2018, revised 26 October 2018, accepted 29 November 2018)

doi:10.1002/1873-3468.13311

Editor: Miguel De la Rosa

The plant-specific protein GIGANTEA (GI) controls many developmental and physiological processes, mediating rhythmic post-translational regulation. GI physically binds several proteins implicated in the circadian clock, photoperiodic flowering, and abiotic stress responses. To understand GI's multifaceted function, we aimed to comprehensively and quantitatively identify potential interactors of GI in a time-specific manner, using proteomics on *Arabidopsis* plants expressing epitope-tagged GI. We detected previously identified (in)direct interactors of GI, as well as proteins implicated in protein folding, or degradation, and a previously uncharacterized transcription factor, CYCLING DOF FACTOR6 (CDF6). We verified CDF6's direct interaction with GI, and ZEITLUPE/FLAVIN-BINDING, KELCH REPEAT, F-BOX 1/LIGHT KELCH PROTEIN 2 proteins, and demonstrated its involvement in photoperiodic flowering. Extending interaction proteomics to time series provides a data resource of candidate protein targets for GI's post-translational control.

Keywords: affinity purification; *Arabidopsis thaliana*; circadian rhythms; flowering time; quantitative mass spectrometry

Arabidopsis thaliana plants have well-documented 24-h rhythms in many physiological processes, from hypocotyl elongation to photosynthetic functions as well as defense responses against pathogen and herbivore attack [1,2]. The overt circadian rhythms are driven by intricate transcriptional-translational feedback loops [2]. Detailed dynamic models based mostly upon transcriptional repression recapitulate the rhythmic expression profiles of these clock genes, including manipulations of the system in mutant plants and under changing photoperiods [3–6].

Gene expression switches can operate on a timescale of minutes. However, it does not obviously explain the slow 24-h timescale of circadian clocks. In addition to chromatin modification [7], the slow degradation rate of the transcriptional repressors extends the timescale of transcriptional regulation, which mathematical analysis has long identified and experiments have confirmed [8,9]. In *Arabidopsis*, regulated protein degradation is also crucial to circadian timing and provides one mechanism for environmental light signals to control the pace of the clock [10].

Abbreviations

3F6H, 3xFLAG-6xHis; MS, mass spectrometry; PCA, principal component analysis; TAP, tandem affinity purification; ZT, Zeitgeber time.

One of the central proteins that regulate the degradation rate of circadian clock proteins in the *Arabidopsis* clock is the GIGANTEA (GI) protein. The *gi* mutants were originally identified as delayed-flowering mutants under long-day conditions where wild-type plants flower early [11,12]. The *gi* mutants also alter the pace of the circadian clock [13–17]. GI affects the clock through interaction with the F-box proteins of the ZEITLUPE (ZTL)/FLAVIN-BINDING, KELCH REPEAT, F-BOX 1 (FKF1)/LIGHT KELCH PROTEIN 2 (LKP2) family, and increases the degradation of the evening-expressed circadian repressors, TIMING OF CAB EXPRESSION 1 (TOC1), and PSEUDO RESPONSE REGULATOR 5 (PRR5) [18–20]. The degradation is directly mediated by the ZTL/FKF1/LKP2 proteins, together with ARABIDOPSIS SKP1-LIKE (ASK) and CULLIN (CUL) proteins, to form an SKP-CUL-F-box (SCF) ubiquitin ligase complex that targets these clock proteins to the proteasome [19–22]. ZTL binds to GI in a light-dependent manner [18]. This interaction stabilizes both ZTL and GI. ZTL is thought to not only enhance GI stability but also to sequester GI in the cytoplasm. GI is rhythmically expressed due to circadian control of *GI* transcription, and therefore GI confers rhythmicity upon ZTL protein levels [23–25]. *GI* mRNA levels peak 8–10 h after dawn [14,26,27], before repression by the evening complex, which are composed of EARLY FLOWERING 3 (ELF3), ELF4, and LUX ARRHYTHMO (LUX, also termed PHYTOCLOCK1) [26,28]. GI protein interacts with and is destabilized by ELF3 and COP1 [29]. Within the nucleus, the clock protein ELF4 interacts with GI and sequesters it away from the promoter of the floral induction gene *CONSTANS* (*CO*), contributing to rhythmic regulation of *CO* [24].

The rhythm of *CO* expression provides part of the timing function required to distinguish long days from short days. *CO* protein activates transcription of *FLOWERING LOCUS T* (*FT*) [30]. GI physically associates with the promoter regions of *CO* and *FT* [31,32], and also binds to transcriptional regulators of *CO* [33]. Morning-expressed *CYCLING DOF FACTOR 1* (*CDF1*), *CDF2*, *CDF3*, and *CDF5* directly repress *CO* and *FT* transcription, delaying flowering in long days [34–36]. The F-box protein FKF1 is co-expressed with GI, binds both to GI and to CDF1–CDF5 under light conditions, and initiates the degradation of CDFs by ubiquitination [34,35]. Thus, GI facilitates expression of *CO* and *FT* at the end of long days, by relieving CDF repression [31,35,36].

In addition to its roles in the clock and flowering, *GI* has been linked to carbon metabolism, [37–39] and various stress responses. *GI* confers tolerance to high

salinity through interaction with the protein kinase SALT OVERLY SENSITIVE 2 (SOS2) [40] and is involved in ELF under drought conditions [41]. Moreover, mutations in *GI* increase resistance to oxidative stress [42] and freezing [43] due to increased CDF expression levels [44]. *GI*'s biochemical mechanisms in most of these responses are unknown.

GIGANTEA's role in the clock is mediated at the biochemical level by co-chaperone activity, which involves binding to HEAT SHOCK PROTEIN 90 (HSP90) and appears to stabilize ZTL [45,46]. This activity can affect other test substrates but its other native targets, if any, are unknown. As outlined above, *GI*'s known functions with the ZTL family and SOS2 are mediated by protein-protein interactions. Therefore, *GI* has been suggested to serve as a scaffold or hub protein that orchestrates other protein interactions [47], for example to provide chaperone activity [46].

Although such protein interactions are thought to mediate *GI*'s functions, these interactions have not been comprehensively and quantitatively analyzed. We therefore conducted interaction proteomics assays using the *GI* protein, and obtained time-resolved data on potential direct and indirect partners of *GI*, over the daily time course. Here, we discuss the abundance profiles of proteins co-immunoprecipitated with *GI*, and functions of new candidate interactors and highlight a DOF protein, which we refer to as CDF6, validating its direct interactions and functional importance.

Materials and methods

Generation of plant materials

To generate plants with epitope-tagged *GI* protein, *gi*-2 mutants were transformed with a construct expressing C-terminal 3xFLAG-6His-tagged *GI* protein (*GI*-3F6H). The full-length *GI* cDNA without the stop codon was amplified and inserted into pENTR/D-TOPO vector (Invitrogen, Carlsbad, CA, USA). After sequence verification, the *GI* cDNA was transferred into the pB7HFC vector, designed for in-frame epitope fusion [48] by a Gateway cloning reaction (Invitrogen). pB7HFC-*GI*-3F6H was introduced to the *gi*-2 mutant by *Agrobacterium*-mediated transformation. Transgenic plants that rescued the *gi*-2 phenotype were selected, and the expression of the *GI*-3F6H protein was verified by western blotting (as in Fig. S1; Methods S1). Samples for the preliminary and qualitative *GI* tandem affinity purification (TAP)-mass spectrometry (MS) studies were prepared as described in [49].

To generate *SUC2:HA-CDF6* plants, the *CDF6* CDS (AT1G26790) was PCR-amplified using cDNA derived from 2-week-old long-day grown plants as a template, and cloned into pENTR D-TOPO (Invitrogen), to form

pENTR HA-CDF6. 2.3 kbp of the *SUC2* 5' upstream promoter region was amplified and cloned into the pENTR 5'-TOPO vector (Invitrogen), to form pENTR 5' *SUC2*. Using a sequential LR clonase II reaction (Invitrogen), we integrated the pENTR 5' *SUC2*, pENTR HA-CDF6 into the R4pGWB501 vector [50], to form *SUC2:HA-CDF6*. After confirming the sequence, this vector was transformed into Col-0 WT plants using by *Agrobacterium*-mediated transformation. Transgenic plants were selected based on the expression level of *CDF6* transcript.

Plant growth conditions

For flowering time experiments, seeds were sown and stratified at 4 °C for 3 days on soil (Sunshine Mix #4; Sun Gro Horticulture, Agavam, MA, USA), containing Osmocote Classic time-release fertilizer (Scotts, Marysville, OH, USA) and Systemic Granules: Insect Control (Bionide, Oriskany, NY, USA). Plants were grown at 22 °C under long-day conditions (16 h light, full-spectrum white fluorescent light bulbs (F017/950/24" Octron; Osram Sylvania, Wilmington, MA, USA, 70–80 $\mu\text{mol}\cdot\text{m}^{-2}\cdot\text{s}^{-1}$). Flowering time was measured as the mean number of rosette leaves, for at least 16 plants per genotype, \pm the standard error of the mean (SEM).

For qPCR analysis, 10-day-old seedlings were grown on 1× Linsmaier and Skoog media (Caisson, Smithfield, UT, USA), supplemented with 3% (w/v) sucrose and 0.8% (w/v) agar, under long-day conditions at 22 °C in growth chambers (CU-36L5; Percival Scientific, Perry, IA, USA; lighting conditions as for flowering time) and harvested at 3-h intervals from 1 h after dawn [Zeitgeber time 1 (ZT1)].

For the preliminary TAP-MS study, growth conditions were the same as for the time series study (see below), and plants were harvested at ZT8. For the qualitative study, plants were grown on soil in long-day conditions (16 h light, 8 h dark) and harvested at ZT13 on day 14. For the TAP-MS time series, GI-3F6H and Col-0 WT seeds were surface-sterilized for 10 min with 30% bleach, 0.01% Triton X-100, followed by four washes with sterile water. After cold-treatment at 4 °C for 5 days, seeds were grown on agar plates [2.15 g·L⁻¹ Murashige & Skoog medium Basal Salt Mixture (Duchefa Biochemie, Haarlem, The Netherlands), pH 5.8] in Percival incubators (CLF Climatics) for 17 days at 85 $\mu\text{mol}\cdot\text{m}^{-2}\cdot\text{s}^{-1}$ (full-spectrum white fluorescent bulbs) and 21 °C in short-day conditions (8 h light, 16 h dark). Seedlings were transferred to soil, for 20 days in the same conditions with a light intensity of 110 $\mu\text{mol}\cdot\text{m}^{-2}\cdot\text{s}^{-1}$. Starting at 7 h after dawn, 80 rosettes without roots were harvested for each replicate, in quintuplicates at time points shown in Fig. 2A and flash-frozen in liquid nitrogen. Dim green safelight was used to harvest samples during darkness. The same total number of WT control samples were harvested as GI-3F6H replicates at each time point, spread out across the time series (leaving out ZT15 and ZT31).

Quantitative PCR (qPCR) analysis

Seedlings were ground into powder with a mortar and pestle with liquid nitrogen, and total RNA was isolated by using an illustra RNAspin Mini kit (GE Healthcare, Chicago, IL, USA) according to the manufacturer's instructions. Two microgram of total RNA was reverse-transcribed using the iScript cDNA synthesis kit (Bio-Rad, Hercules, CA, USA) according to the manufacturer's instructions. cDNA was diluted five times with water, and 2 μL was used as a template for quantitative PCR (qPCR) analysis using primers as shown in Table S1. *ISOPENTE-NYL PYROPHOSPHATE/DIMETHYLALLYL PYROPHOSPHATE ISOMERASE 2 (IPP2)* was used as an internal control for normalization. The average value from WT was set to 1.0 to calculate the relative expression of other lines. To amplify *CO* and *CDF6*, three-step PCR cycling program was used: 1 min at 95 °C, followed by 40–50 cycles of 10 s at 95 °C, melting temperatures for 15 or 20 s, and 72 °C extension for 15 s. To amplify *GI*, *FT*, and *IPP2*, a two-step PCR cycling program was used: 1 min at 95 °C, followed by 40–50 cycles of 10 s at 95 °C and 20 s at 60 °C. Data show the average of three biological replicates with SEM; each measurement had two technical replicates.

Protein Extraction and tandem affinity purification (TAP) procedure

All steps in the protein extraction, TAP, and preparation for MS were carried out in random sample order to avoid bias due to order of processing. Frozen plant tissue was ground to a fine powder in a liquid nitrogen and dry ice-cooled mortar and processed essentially as described [49]. Detailed procedures are described in Supporting Experimental Procedures (Methods S2).

Protein digestion and mass spectrometric analysis

Preparation of samples for MS for the qualitative and time series studies analysis used an on-bead digest, prior to mass spectrometric analysis. Detailed procedures are described in Supporting Experimental Procedures (Methods S3).

Proteomics data analysis and bioinformatics

For the qualitative study, database searches were performed using Comet [51], searching against the Uniprot *Arabidopsis* protein sequence database, and using Percolator (Matrix Science, Boston, MA, USA) with a *q*-value cut-off of 0.01. Cysteine residue masses were considered statically modified by iodoacetamide, and methionine dynamically modified by a single oxidation. Precursor mass tolerance was 10 p.p.m., and product ion tolerance was 0.5 Da. The principle of parsimony was used for protein

inference, and at least two unique peptides were required for each identified protein.

The time series data were analyzed using the commercial Progenesis LC-MS software (version 4.1.4924.40586; Nonlinear Dynamics, Newcastle, UK) for label-free quantitation. Raw files were imported into a label-free analysis experiment, chromatograms were subjected to automatic alignment and peak picking. Only charges 2+, 3+, and 4+ and data from 25 to 75 min of the runs were chosen for analysis. The exported file of MS/MS spectra was uploaded on the Mascot website (version 2.4) and a search was carried out with the following parameters: database *Arabidopsis*_1rep (version 20110103), trypsin as enzyme, allowing up to two missed cleavages, carbamidomethyl (C) as a fixed modification, Oxidation (M), Phospho (ST) and Phospho (Y), as variable modifications, a peptide tolerance of 10 p.p.m., and MS/MS tolerance of 0.05 Da, peptide charges 2+, 3+, and 4+, on a QExactive instrument (Thermo, Waltham, MA, USA), and with decoy search to determine false discovery rate (FDR). For export, an ion-cutoff of 20 was chosen (exported peptide measurements: Data S9). The MS proteomics data have been deposited to the ProteomeXchange Consortium (<http://proteomecentral.proteomexchange.org>) via the PRIDE partner repository [52] with the dataset identifier PXD006859. Technical outliers were identified using correlation analysis and principal component analysis (PCA) of protein abundance data implemented by an R script (Data S5). The average Pearson correlation coefficient of each *GI*-TAP replicate with the other replicates of the same time point was above 95% for all *GI*-3F6H samples apart from sample 19E (Fig. S2), which was also clearly separated from all other samples by PCA and was therefore discarded.

A custom R script performed further statistical analysis and plotting (Data S7). We used a *t*-test to determine for each protein, whether the maximum *GI*-TAP time point (omitting the 31-h time point) is significantly different from the WT control average using *q*-values [Benjamini-Hochberg (BH) corrected *P*-values]. ‘Fold enrichment’ is the ratio of the highest *GI*-TAP time point to the WT control average gives. To assess temporal changes, ANOVA was performed on arcsinh-transformed *GI*-TAP data, including the ZT 31 time point. To assess rhythmicity, we used the JTK_CYCLE tool [53] to analyze periods of 22–26 h (Data S8). The summary heatmap (Fig. 2D) used the heatmap.2 function of the pvclust v2.0 R package [54]. Gene ontology (GO) analysis was performed using topGO (<http://bioconductor.org/biocLite.R>, version: 2.16.0, [55,56]), using a node size of 3, as described by [57] (Data S6). Biological context was provided by subcellular locations annotated in the SUBA resource [58] and interaction data in the BioGrid [59].

Yeast two-hybrid assay

Full-length *CDF6* coding sequence was PCR-amplified using cDNA as template with primers shown in Table S1,

cloned into pENTR/D-TOPO (Invitrogen) and sequence-verified. The plasmid cassette was transferred to pAS-GW, a gateway compatible bait vector [60] using LR clonase II (Invitrogen). The *GI*-FL, *GI*-N, *GI*-M + C, FKF1, LKP2, and ZTL clones used in this analysis were described previously; *GI*-FL, *GI*-N and *GI*-C [31], and FKF1, LKP2, and ZTL [34]. Yeast strains Y187 and AH109 were transformed with prey and bait vectors, respectively using the standard yeast transformation protocol (Clontech, Mountain View, CA, USA). After colonies formed on –W or –L containing media, three independent colonies were grown together, and then mated against their corresponding pairs for 3 days on YPDA media. After mating, yeast colonies were transferred onto –WL media. After checking for mating confirmation, yeast sectors were retransferred at the same time onto –WL and –WLH media. The experiments were repeated several times with the same results.

Modeling methods

Simulations of the P2011 clock model [5] for *GI* and *GI*-3F6H were performed in COPASI v4.16 [61]. Simulations of the Framework Model FMv2 [62] for *CO*, *FT*, and flowering time were performed in MATLAB (Mathworks, Cambridge, UK). Both models are available online: P2011 (http://www.plasmo.ed.ac.uk/plasmo/models/download.shtml?accession=PLM_71&version=1) and FMv2 (<https://figshare.com/articles/248?version=2>). The higher arrhythmic *GI* RNA levels in *GI*-3F6H plants were simulated by reducing the affinity of *GI* for its rhythmic transcriptional inhibitors (parameters *g14*, *g15*) by 100-fold each, compared to the default, wild-type values. Transcriptional activation (parameter *n12*) was then reduced by 36% to match the observed *GI*-3F6H mRNA level. The effects on other model readouts (Figs 1 and 3) were caused by this simulated transcriptional mis-regulation of *GI*. Simulations of the flowering pathway were conducted using the photoperiod and temperature conditions of the corresponding experiments.

Results

Characterization of the *GI*-3F6H transgenic plant line

We transformed the strong *gi*-2 mutant (a deletion allele predicted to truncate ~90% of *GI* protein) [14] with a construct to express 3xFlag- and 6xHis-tagged *GI* protein under the control of the CaMV 35S promoter (*GI*-3F6H). We aimed to express *GI*-3F6H protein constitutively at a similar level throughout the day to be able to immunoprecipitate a similar amount of *GI* at each time point [31]. This will enable us to detect the changes in interaction of certain proteins

with GI rather than the changes in the amount of co-immunoprecipitated proteins caused by the different amount of GI expressed. After isolating several positive transformants, we chose the line in which the expression levels of *GI-3F6H* transcripts were similar to the peak expression levels of the endogenous *GI* (Fig. 1A). As a first experiment, we performed a preliminary study where we used TAP of *GI-3F6H* followed by silver-staining of a protein gel separation and LC-MS of excised gel bands (Fig. 1F, Fig. S1, Data S1). Our *GI-3F6H* line expressed sufficient GI protein for effective TAP and analysis of gel bands by MS identified GI and known interactors (Fig. S1, Data S1). In addition, this *GI-3F6H* construct completely rescued the late flowering phenotype of *gi-2*, indicating that *GI-3F6H* is functional (Fig. 1B). In the *GI-3F6H* line, *CO* and *FT* mRNAs were higher than in the WT in the morning (Fig. 1C,D), consistent with activation of these flowering-promoting genes by GI in the light [31,32]. This was also reflected by slightly ELF of the *GI-3F6H* plants relative to the WT (Fig. 1B).

GIGANTEA has multiple, known effects on the clock and flowering genes and proteins; several of these effects have been incorporated into mathematical models [5,62]. In order to test whether the effects of the mis-regulated *GI-3F6H* transgene were replicated by these known mechanisms, we simulated the rescued mutant line in the *Arabidopsis* Framework Model version 2 [62], a mechanistic, mathematical model that includes photoperiodic flowering (Fig. 1B,E). The WT and *gi-2* simulations closely matched the mRNA data. This data set favored morning (1–4 h after dawn) expression of *CO* and *FT* compared to evening (13–16 h) expression slightly more than the model, possibly reflecting a reduced *GI* mRNA level at 13 h in this data set compared to previous training data. The model correctly predicted an elevated *CO* mRNA level at 1 h in *GI-3F6H* plants, though the observed level was ~5-fold rather than ~2-fold higher (Fig. 1C). This *CO* peak induced more *FT* at 4 h in the model (Fig. 1E) than in the plant (Fig. 1C), and therefore earlier flowering (Fig. 1D). Morning regulation of *FT*, in the presence of unusually high GI levels, differed most between the model and the plant, highlighting this as an area for future model refinement.

Next, *GI-3F6H* and WT plants (control) were grown in long days for 2 weeks and harvested at ZT 13 when GI protein peaks [31] and potential GI-interacting proteins were identified in a qualitative proteomics study (Fig. 1F). TAP of *GI-3F6H* was carried out, followed by on-bead digestion and qualitative MS analysis (Fig. 2B), reporting peptide counts (Fig. 1F). Fifty *Arabidopsis* proteins were identified by at least

one peptide in each of the *GI-3F6H* samples and none in the controls. In order to exclude known nonspecific interactors, we eliminated all proteins from our list that were previously reported to be purified by GFP-3F6H with the same sample preparation protocol [48] (Data S3). In addition, during the extraction, *GI-3F6H* can come in contact with proteins from compartments that are inaccessible to it in an intact cell. Therefore, we also excluded proteins from further analyses that are located in the chloroplast or mitochondria but not in the cytoplasm or nucleus according to their GO annotation [63] (Table 1; full results in Data S2). Eighteen proteins remained after this background removal strategy, indicating the potential to identify previously undiscovered interactions, as discussed below. Detection of known direct interactors, such as ZTL, FKF1, and LKP2, as well as indirect interactors, ASK1 and ASK2 (direct interactors of ZTL and FKF1) validated the methodology [16,21,31,64].

Candidate GI-interacting proteins from time series data

Although GI plays an important role in photoperiodic flowering in long days, the function of GI under short-day conditions remains elusive. Therefore, we grew plants in short days to identify uncharacterized interactors of GI potentially involved in other responses. In order to obtain time-resolved interaction data, we applied the same GI-TAP method as in the qualitative study to plants grown in short-day conditions, at six time points in biological quintuplicate, with additional duplicate samples at time point 31 h (replicating the 7-h time point; Fig. 1F ‘time series’, Fig. 2A). Short-day conditions ensure plants to be at a vegetative stage at the time of sampling, while being large enough to obtain sufficient amounts of tissue from a manageable number of plants for our time-resolved TAP-MS procedures. Extraction, TAP, and sample preparation for MS were carried out as for the qualitative analysis (Fig. 2B). Using the Mascot search engine to identify peptides, our choice of peptide score cutoff of 20 resulted in an FDR of 0.023. After identification and quantification of proteins (Fig. 2C), one outlier (*GI-3F6H* sample at ZT19, replicate E) was excluded from subsequent analysis (see Experimental Procedures; Fig. S2). PCA of the remaining GI samples maximally separated the mid/late-night time points 19 h and 23 h from mid-day time points 7 h and its replicate 31 h (Fig. 2E).

Two thousand three hundred thirty-six peptides were detected in the time series study, from which 500 proteins were quantified (Table 2). In order to exclude known unspecific interactors, we used the same

Table 1. Candidate interacting proteins identified in the qualitative study. Control (WT samples) and GI-3F6H samples were extracted in RIPA or SII buffer. Eighteen *Arabidopsis* proteins were identified by at least one peptide in each GI-TAP sample and none in the WT background controls, excluding proteins that are likely contaminants as they bind to GFP-3F6H [48] or localized to other compartments than GI (chloroplast, mitochondria). The right-hand columns cross-reference the time series study (Table 3), with fold enrichment and significance (*q*-value) of the maximum GI-3F6H time point relative to the WT control. Bold: known direct or indirect interactors and homologs. n.d.: not detected.

Accession	Name	Number of peptides identified in qualitative TAP experiment		GI-3F6H time series enrichment (max. GI/WT)	
		GI TAP RIPA	GI TAP SII	<i>t</i> -test <i>q</i> -value	Fold enrichment
AT1G22770	GIGANTEA	309	299	0.00030	76
AT5G57360	ZTL	47	61	0.00020	32
AT5G06600	UBP12	15	20	0.00022	19
AT3G13920	EIF4A1	5	10	n.d.	n.d.
AT1G68050	FKF1	6	9	0.00038	12
AT2G18915	LKP2	6	9	0.00074	13
AT1G75950	ASK1	7	8	0.0011	8.6
AT3G08530	CHC2	1	5	0.43 ^a	2.44
AT5G60390	EFTu/EF1-A	4	2	n.d.	n.d.
AT2G44060	At2G44060	3	2	n.d.	n.d.
AT5G42190	ASK2	2	2	n.d.	n.d.
AT3G56340	RPS26E	1	3	n.d.	n.d.
AT4G03550	CALS12	1	1	n.d.	n.d.
AT1G70490	ARF2-B	1	1	n.d.	n.d.
AT1G80870	AT1G80870	1	1	n.d.	n.d.
AT2G29420	GSTU7	1	1	n.d.	n.d.
AT3G58350	RTM3	1	1	n.d.	n.d.
AT5G23540	AT5G23540	1	1	0.17 ^a	1.88 ^a

^aBelow threshold in time series study.

strategy as for the qualitative study, eliminating 80 proteins previously purified by GFP-3F6H [48] and 169 chloroplast and mitochondrial proteins [63] (Data S3, S4 and S6). The analytical methods also quantified the identified peptide peaks in WT control samples (one replicate for each time point except ZT 15 and ZT 31) that had been subjected to the same TAP procedure (Figs 1F and 2A). Subsequent analysis used raw abundance data exported from Progenesis as opposed to the abundance which is normalized by the sum of all intensities of ions with the chosen inclusion criteria (see Materials and methods) in each mass spectrometric analysis; however, analysis of normalized data gave very similar results (data not shown and Data S3). The fold enrichment of each protein in the GI-3F6H was calculated as the peak GI-3F6H abundance relative to the average abundance in the WT control samples. Potential interacting proteins were identified as significantly enriched by *t*-test compared to the WT control, with a significance threshold adjusted for multiple testing (BH-adjusted *q*-value < 0.05). Fold-enrichment threshold values were informed by the results for known interactors. The direct interactors ZTL, FKF1, and LKP2 were more than 10-fold enriched over the WT control in the GI-

3F6H time series. Indirect interactors CUL1/CUL2 and GLUTAMINE SYNTHETASE 2 (GLN2) [21,49] were two- to three-fold more abundant at their peaks than the time series control and were not identified in the preliminary or qualitative studies. Hereafter, we refer to significantly enriched proteins with at least four-fold enrichment as highly enriched (55 proteins) and to proteins with two- to four-fold enrichment as weakly enriched (a further 88 proteins).

Among these 88 proteins, 13 changed significantly in abundance within the time series (assessed for any change by ANOVA, *q*-value < 0.05) or 10 as assessed for rhythmic profiles (by JTK_CYCLE *q*-value < 0.05; Table 2 and Data S3; Data S8). Peak abundance for most of the 16 proteins with changing or rhythmic precipitated protein abundance, as well as nonrhythmic/changing precipitated proteins occurred at 7 h, with lowest average abundance at 23 h among the significantly enriched proteins, and no rhythmic or changing proteins peaking at 15 h (Fig. 2D,E). The immunoprecipitated abundance of GI changed about two-fold over time (Fig. 3A). The observed abundance changes for immunoprecipitated GI and ZTL closely matched the predicted protein profiles (Fig. 3C) from simulation of GI-3F6H (as in Fig. 1E). This result indicated

Table 2. Numbers of quantified and significant proteins in the GI-3F6H-MS time series. The raw data of the Progenesis output file and the raw data after removing likely unspecific proteins (GFP interacting proteins [48]) and plastid or mitochondrial proteins, (see Data S3) was used for statistics.

	1 or more unique peptides	Of these, JTK_CYCLE <i>q</i> -value < 0.05	2 or more unique peptides	Of these, JTK_CYCLE <i>q</i> -value < 0.05
Total quantifiable identifications	500	43	231	17
Without GFP interactors	420			
Without plastid/mitochondrial proteins	251	32	88	9
Of these 251 (1 or more unique peptides) or 88 (2 or more unique peptides):				
Significantly enriched (BH <i>q</i> -value < 0.05) ^a	91	10	36	3
And fold enrichment > 2	88	10	33	3
And fold enrichment > 4	55	8	18	2

^aThese numbers exclude proteins where t-test was impossible due to missing quantifications.

that the multiple mechanisms of GI and ZTL protein regulation in the model were sufficient to replicate the abnormal accumulation of GI-3F6H protein, and its effects on ZTL. The change in precipitated GI abundance was not significant by ANOVA or JTK_CYCLE.

Functional categorization of GI-TAP enriched proteins

Gene ontology analysis was done, using the candidates in Table 3 as foreground. GO terms related to protein degradation were overrepresented among the candidates, as well as light response related terms, some metabolic processes, and flower development (Data S4 and S6).

Rhythmic profiles of known interactors

In contrast to the weakly rhythmic trend in abundance of the immunoprecipitated GI protein, known interactors showed contrasting profiles (Fig. 3A). The direct interactors FKF1, ZTL, and LKP2 showed temporal profiles consistent with their mRNA expression patterns [65–68] (Fig. S3). The ZTL profile paralleled GI, consistent with their mutual stabilization [23] and closely matched by the prediction from the model simulation (Fig. 3C). Co-immunoprecipitated LKP2 abundance had a similar trend, consistent with arrhythmic mRNA expression of ZTL and LKP2. Only FKF1 and CDF3 were strongly rhythmic, with FKF1 peaking at 7–11 h, resembling previous data [35,69] and CDF3 peaking at 27 h. Therefore, CDF3 level is in antiphase with FKF1, in line with the degradation of CDFs by FKF1 [34,35]. These results demonstrate the consistency of our data with published results. CDF3 was quantified using a single, individually inspected peptide, indicating that such data should not be excluded from analysis.

Several established indirect interactors of GI were quantified (Fig. 3A). CDF3 and GLN2 are client proteins of FKF1 [49], with CDF3 also being a direct GI interactor (see above) [31], whereas ZTL and LKP2 also interact with the core components of the SCF ubiquitin E3 ligase detected here, ASK1 and CUL1 and/or CUL2 (closely related proteins that were not distinguished by the peptides detected).

The predicted functions of candidate interactors include protein degradation and stabilization

In addition to verifying the known indirect interactor CUL1, our analysis enriched other proteins involved in protein stability (Fig. 3B). The ubiquitin-specific proteases (UBP) 12 and UBP13 (AT5G06600 and AT3G11910) were enriched in the time series and qualitative studies. Both UBP12 and UBP13 regulate the period length of the circadian clock as well as photoperiodic flowering [70], therefore the function of UBP12 and UBP13 in the clock and flowering regulation might be through the GI complex (see note added in proof). AAA-type ATPase family proteins related to components of the 26S proteasome (AT1G45000 and/or AT4G27680) and a protease inhibitor, CYSTATIN 1 (AT5G12140) were also enriched. Several proteins annotated as being involved in protein stabilization were also significantly enriched by GI-3F6H, such as Cpn60 chaperonin family proteins (AT1G24510, AT3G18190, AT3G02530 and AT3G03960), the putative co-chaperone TPR4 (AT1G04530; Table 3, Fig. 3B) and at least one HSP90 (AT5G56030, AT5G52640 and/or AT5G56000, Fig. 3B). HSP70 family proteins were just below the enrichment cutoff (Table 3).

In contrast, neither additional F-box proteins nor other proteins involved in circadian timekeeping were identified as strong candidate interactors (enrichment

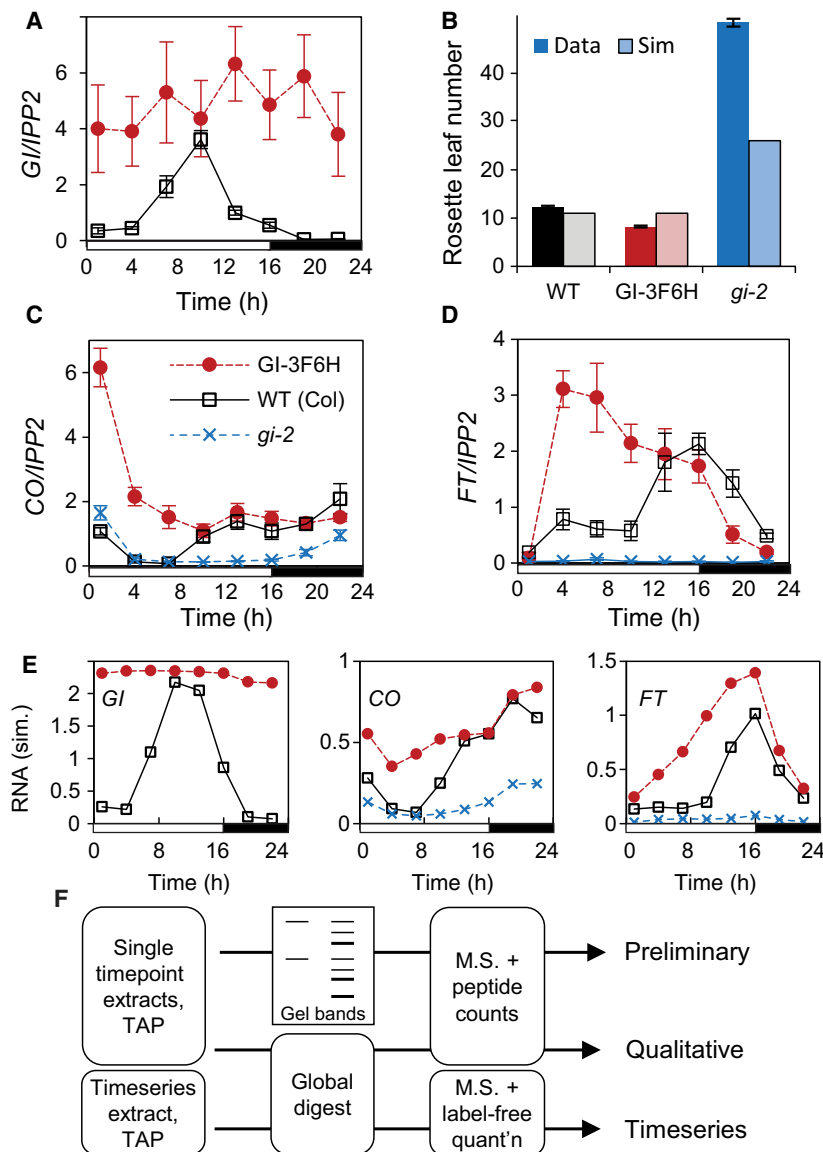


Fig. 1. Evaluation of the *GI-3F6H* complementation line. (A,C,D) mRNA expression was tested in samples of *Arabidopsis* plants of the Col-0 WT (black open squares), *gi-2* mutant (blue crosses) and *gi-2* plants constitutively expressing the *GI-3F6H* fusion protein (red filled circles) under long-day conditions. qPCR assays detected *GI* (A), *CO* (C) or *FT* (D) mRNA. Data are means of biological triplicates, normalized to an *IP2* internal control; error bar, SEM. (B) Rosette leaf number was measured (data in bold) at flowering time in *GI-3F6H*, with WT and parental *gi-2* mutant controls, under long-day conditions. The flowering experiment was simulated using the FMv2 (pale colors). Data are averages of 16 plants; error bar, SEM. (E) *GI* transcription in the FMv2 was adjusted to match the *GI* mRNA profile of *GI-3F6H* in (A); predicted expression profiles of *CO* and *FT* are shown (as in C, D). (F) Overview of proteomics studies using *GI-3F6H*.

of PRR3 in the time series was below the significance threshold). Multiple, metabolic enzymes and translation elongation or initiation factors were enriched in the *GI-3F6H* time series. Among those (Table 3), were GTP-binding translation factors (AT1G72730 and AT1G54270 and/or AT3G19760), TREHALOSE-6-PHOSPHATASE SYNTHASE 8 (TPS8; Fig. 3B), a phosphofructokinase family protein (AT1G20950) and a GMP synthase homolog (AT1G63660, Table 3) and a pyruvate kinase family protein (AT2G36580). In addition, a protein that binds to di- or trimethylated histone H3, ALFIN-LIKE 7 (Table 3) was enriched by *GI-3F6H*. The candidate interactors suggest new clients and mechanisms of *GI* action related to those in

other species (see Discussion), though their physiological significance awaits confirmation.

CDF6 is a *GI* interactor that contributes to photoperiodic flowering

AT1G26790 encodes a predicted DOF transcription factor that was up to 15-fold enriched around dawn in our *GI-3F6H* time series results (23 h and 27 h; Fig. 4A). This protein was the most significantly rhythmic of the candidate interactors after FKF1 and CDF3 (BH-adjusted *P*-value from JTK_CYCLE = 8×10^{-6}). Its immunoprecipitated protein levels were the most anticorrelated with FKF1 levels among the

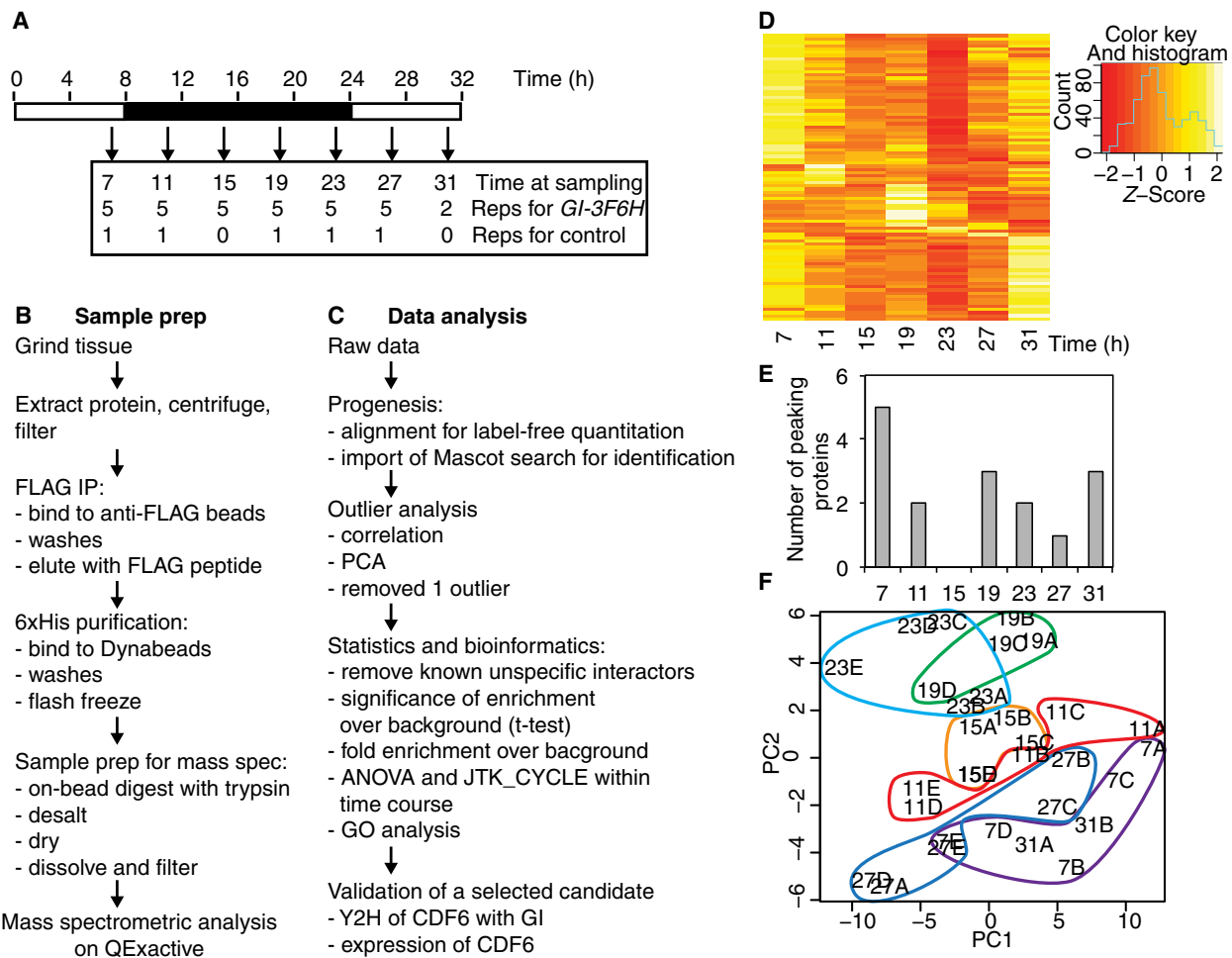


Fig. 2. GI-TAP time series. (A) Samples from GI-3F6H transgenic plants and WT control plants grown in short-day conditions were harvested at the indicated time points and replication. (B) Workflow for protein extraction, TAP using FLAG and His tags, and peptide preparation for MS. (C) Workflow for label-free, quantitative data analysis, statistical and bioinformatics tests. (D) Heat map of protein abundance over time for 88 proteins with significant enrichment of at least two-fold (excluding proteins that bind to GFP or are only found in inaccessible compartments). (E) Distribution of peak times, for 16 proteins shown in (D) with significant change over the GI-3F6H time course (ANOVA $q < 0.05$ or JTK_CYCLE $q < 0.05$). (F) PCA separates GI-TAP time points (grouped by number and contour, with replicate letter, all quantified proteins used) over components 1 and 2 (PC1, PC2). Note 31 h time point replicates 7 h.

highly enriched proteins (Fig. 4A), followed by CDF3 ($r = -0.65$ and -0.40 , respectively). The DOF protein AT1G26790 is a close homolog of CDF5 [35,71] and its mRNA expression showed a robust circadian oscillation in constant light (Fig. 4C). Therefore, we named this gene *CYCLING DOF FACTOR 6* (*CDF6*). We then validated the interaction of CDF6 with GI and ZTL/FKF1/LKP2 proteins as well as its function. Yeast-2-hybrid (Y2H) assay experiments confirmed the interaction of full-length, N-terminal, and C-terminal regions of GI with CDF6, as well as interaction of CDF6 with FKF1, ZTL, and LKP2 (Fig. 4B). *CDF6* transcript abundance was tested in plants transferred to constant light, revealing

circadian regulation with a sharp peak around subjective dawn (Fig. 4C), similar to *CDF1* transcript abundance [34,67] and the profile of CDF6 in the GI-3F6H time series (Fig. 4A).

Since GI interacts with FKF1 and most likely CDF3 [31,35] (Fig. 3A), and because the CDF6 amino acid sequence shows high similarity to other CDFs, we predicted that CDF6 also has a similar function to other CDFs. To assess our hypothesis, transgenic plant lines were generated, in which *CDF6* was expressed from the *SUCROSE-PROTON-SYMPORter* (*SUC2*) promoter that is active in phloem companion cells [36]. We chose the *SUC2* promoter to drive *CDF6*, because other CDFs as well as likely target genes of CDF6 – *CO* and

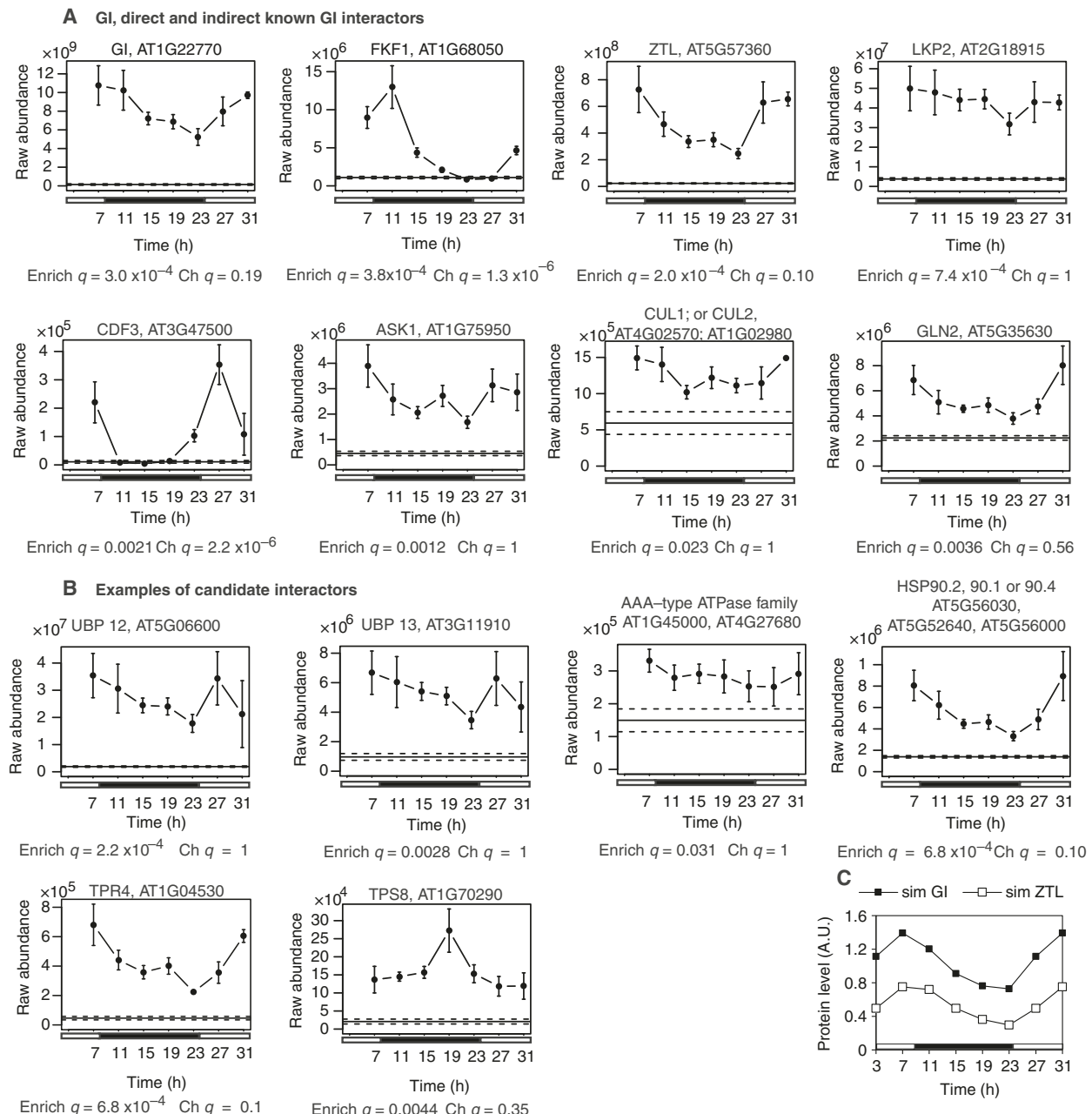


Fig. 3. Diel profiles of immunoprecipitated GI and interacting proteins. Immunoprecipitated protein abundance of (A) GI and direct and indirect interactors detected in the time series study, along with (B) HSP90 and candidate direct or indirect interactors. Multiple gene identifiers indicate related proteins were not distinguished by the three CUL or five HSP90 peptides detected. GI-3F6H samples, markers; error bar, SEM. Average of WT control, horizontal line, \pm SEM, dashed line. Time (T); Significance of enrichment and temporal change are shown, as q -values of t -test comparing GI-TAP peak to WT (Enrich q) and of JTK_CYCLE within the GI TAP-MS time series (Ch q). Biological replicates in (A and B): 5, except for ZT 19 (four replicates) and ZT 31 (two replicates). (C) Simulation of the GI and ZTL protein time series, using the model matched to GI-3F6H RNA data (Fig. 1E) under short-day conditions, closely matches observations (panel A).

FT – are specifically expressed in phloem companion cells [72,73]. Two lines, *SUC2:HA-CDF6* #8 and #11, accumulated higher levels of the *CDF6* transcript at

ZT4 and in later time points of a qPCR time series (Fig. 4E), fluctuating around 20–60% of the WT peak level, whereas *CDF6* levels in WT were very low except

Table 3. Known and candidate interactors of GI from GI-3F6H TAP-MS time course experiment. Quantified proteins with two or more peptides that were significantly enriched (in t-test of maximum GI-TAP time point with WT control q -value < 0.05) by at least two-fold (max. GI-TAP/WT > 2), ranked by fold enrichment. Only FKF1, CDF3 and CDF6 were rhythmic (JTK_CYCLE q -value < 0.05). Where peptides matched very similar proteins, multiple accession numbers are shown. Bold type, known direct or indirect interactors. Detection in the preliminary study (Prelim., Fig. 1F) is shown, and the sum of peptide numbers detected in the qualitative study (Qual., Fig. 1F) in GI-3F6H and WT (control). Selected proteins detected by single peptides are shown below, along with proteins suggested by other hypotheses (see Discussion) that were below thresholds in the time series (*) but were detected in the qualitative study. Likely unspecific interactors [48] and inaccessible proteins are left out in this table.

Accession	Name	Quantitative enrichment (max GI TAP/control)					Prelim. study Detected? (Y/n)	Qual. study Total peptides, GI-TAP/control
		Time series, number of peptides	t-test (P-value)	t-test BH adjusted (q -value)	Max GI/control			
≥ 2 peptides per protein								
AT1G22770	GIGANTEA	59	6.2E-06	3.0E-04	76	Y	608/0	
AT5G57360	ZTL	29	2.5E-06	2.0E-04	32	Y	102/0	
AT5G06600	UBP12	9	3.60E-06	2.17E-04	19	Y	35/0	
AT1G04530	TPR4	2	2.70E-05	6.80E-04	15	Y	n.d.	
AT2G18915	LKP2	18	3.4E-05	7.4E-04	13	Y	15/0	
AT4G36250	ALDH3F1	2	4.13E-05	8.30E-04	12	n	n.d.	
AT1G68050	FKF1	9	1.3E-05	3.8E-04	12	Y	15/0	
AT5G54770	THI1	2	0.00051	0.0044	11	n	n.d.	
AT5G22800	EMB86	3	6.33E-05	0.0011	11	n	n.d.	
AT1G74730	DUF1118	2	0.00031	0.0030	7.6	n	n.d.	
AT3G11910	UBP13	7	2.76E-04	0.0028	6.9	Y	n.d.	
AT5G38660	APE1	3	5.27E-04	0.0044	6.5	n	2/0	
AT3G60750; AT2G45290	Transketolase	9	0.0060	0.023	6.5	n	n.d.	
AT5G56030; AT5G52640;	HSP90.2; HSP90.1;	5	2.8E-05	6.8E-04	6.4	n	n.d.	
AT5G56000	HSP90.4							
AT3G02530	TCP-1/cpn60 chaperonin	2	1.08E-04	0.0015	5.6	n	n.d.	
AT3G03780	MS2	2	5.44E-04	0.0044	5.6	n	n.d.	
AT1G18080	RACK1A	2	4.06E-04	0.0038	5.1	n	n.d.	
AT3G03960	TCP-1/cpn60 chaperonin	2	0.0022	0.011	5.1	n	n.d.	
AT1G07410; AT1G01200	RAB-A2B	2	0.010	0.032	3.8	n	n.d.	
AT1G54270; AT3G19760	EIF4A-2	2	0.0027	0.013	3.7	Y	n.d.	
AT5G46290	KASI	3	0.0014	0.0082	3.6	Y	1/0	
AT5G35630	GS2	5	7.13E-04	0.0054	3.6	n	2/0	
AT5G60790; AT3G54540	GCN1	3	0.0088	0.031	3.4	n	n.d.	
AT2G28000	CPN60A	2	0.0022	0.011	2.9	n	n.d.	
AT1G78570	RHM1	2	0.0014	0.0082	2.8	n	n.d.	
AT2G36880; AT1G02500	MAT3	2	0.0013	0.0081	2.8	n	n.d.	
AT2G21330; AT2G01140	FBA1	2	0.0022	0.011	2.7	n	n.d.	
ATCG00820	RPS19	2	0.0021	0.011	2.6	n	n.d.	
AT1G20620	CAT3	11	0.0040	0.018	2.5	Y	n.d.	
AT4G02570; AT1G02980	CUL1	3	0.010	0.031	2.5	n	n.d.	
AT3G42050	Vacuolar ATP synthase subunit H	2	0.0014	0.0082	2.4	n	3/18	
AT2G37270	RPS5B	2	0.013	0.037	2.3	n	n.d.	
AT2G09990; AT3G04230	Ribosomal protein S5	4	0.018	0.048	2.1	n	n.d.	
≥ 1 peptides per protein (selection)								
AT5G10450	GRF6	1	1.3E-05	3.8E-04	90	n	n.d.	
AT1G60780	HAP13	1	0.011	0.034	58	n	n.d.	
AT3G47500	CDF3	1	2.4E-04	0.0026	33	n	n.d.	
AT1G14510	AL7	1	4.7E-05	8.7E-04	18	n	n.d.	

Table 3. (Continued).

Accession	Name	Quantitative enrichment (max GI TAP/control)					Prelim. study Detected? (Y/n)	Qual. study Total peptides, GI-TAP/control
		Time series, number of peptides	t-test (P-value)	t-test BH adjusted (q-value)	Max GI/control			
AT3G14420.1; AT4G18360	Aldolase-type TIM barrel	1	0.0089	0.031	17	n	n.d.	
AT1G26790	CDF6	1	0.0010	0.0068	15	n	n.d.	
AT3G13470	TCP-1/cpn60 chaperonin	1	0.018	0.048	15	n	4/0	
AT1G70290	TPS8	1	5.4E-04	0.0044	13	n	n.d.	
AT5G12140	CYS1	1	2.6E-04	0.0027	10	n	1/0	
AT1G20330	SMT2	1	1.5E-04	0.0017	9.1	n	n.d.	
AT4G11150	TUF	1	0.0013	0.0081	8.8	n	5/10	
AT1G75950	ASK1	1	7.2E-05	0.0011	8.6	n	13/0	
AT2G16570	ASE1	1	0.0082	0.030	8.1	n	n.d.	
AT2G33040	ATP3	1	0.0094	0.031	7.8	n	n.d.	
AT1G24510	TCP-1/cpn60 chaperonin	1	7.9E-04	0.0057	7.3	n	n.d.	
AT3G18190	TCP-1/cpn60 chaperonin	1	1.4E-04	1.7E-03	7.0	n	n.d.	
AT1G72730	DEA(D/H)-box RNA helicase	1	6.7E-05	0.0011	7.0	n	n.d.	
AT1G53750	RPT1A	1	0.0096	0.031	6.6	n	n.d.	
AT4G31420	REIL	1	0.0020	0.011	6.6	n	n.d.	
AT5G28050	Cytidine/deoxycytidylate deaminase	1	1.3E-04	0.0017	5.1	n	n.d.	
AT1G29880	glycyl-tRNA synthetase	1	0.0010	0.0068	4.9	n	n.d.	
AT5G51110	Transcriptional coactivator	1	6.8E-04	0.0053	4.8	n	n.d.	
AT5G01410	PDX1	1	0.0096	0.031	4.7	n	n.d.	
AT3G60300	RWD domain-containing	1	0.012	0.037	4.4	n	n.d.	
AT5G58140	PHOT2	1	0.0087	0.031	3.5	n	n.d.	
AT4G38630	RPN10	1	0.014	0.041	3.3	n	n.d.	
AT4G25630	FIB2	1	0.0052	0.022	3.0	n	n.d.	
AT1G48630	RACK1B_AT	1	0.0059	0.023	2.9	n	n.d.	
AT1G56110	NOP56	1	0.014	0.041	2.7	n	n.d.	
AT1G20200	EMB2719	1	0.0050	0.022	2.4	n	2/1	
AT5G41210	GSTT1	1	0.018	0.048	2.3	n	n.d.	
AT3G20050	TCP-1	1	0.0098	0.031	2.2	n	2/0	
AT1G63660	GMP synthase	1	0.0097	0.031	2.2	n	n.d.	
AT1G45000.1; AT4G27680	AAA-type ATPase	1	0.0097	0.031	2.2	n	n.d.	
GFP-TAP binding but found in time series and qualitative study and not background of qualitative study								
AT3G17390	SAM4	2	0.0058	0.016	1.9*	n	3/0	
AT5G17920	MS1	4	0.056*	0.095*	1.8*	n	7/0	
AT5G02500; AT1G16030; AT1G56410; AT3G09440; AT3G12580; AT5G02490; AT5G28540	Hsp70 family		0.053*	0.26	2.52	n	13/0	

at the ZT1 peak. Both transgenic lines flowered significantly later than WT under long photoperiods, with less effect under short photoperiods (Fig. 4D). If CDF6 acts in a similar way to CDF1 [36,71], we would expect it to inhibit transcription of both *CO* and *FT*. Indeed, *CO*

mRNA levels were reduced at 10, 13 h and at night in the transgenic plants compared to WT, and *FT* expression was reduced more than 10-fold at 4 h and at later time points (Fig. 4E). These results are consistent with CDF6 participating in the photoperiodic regulation of

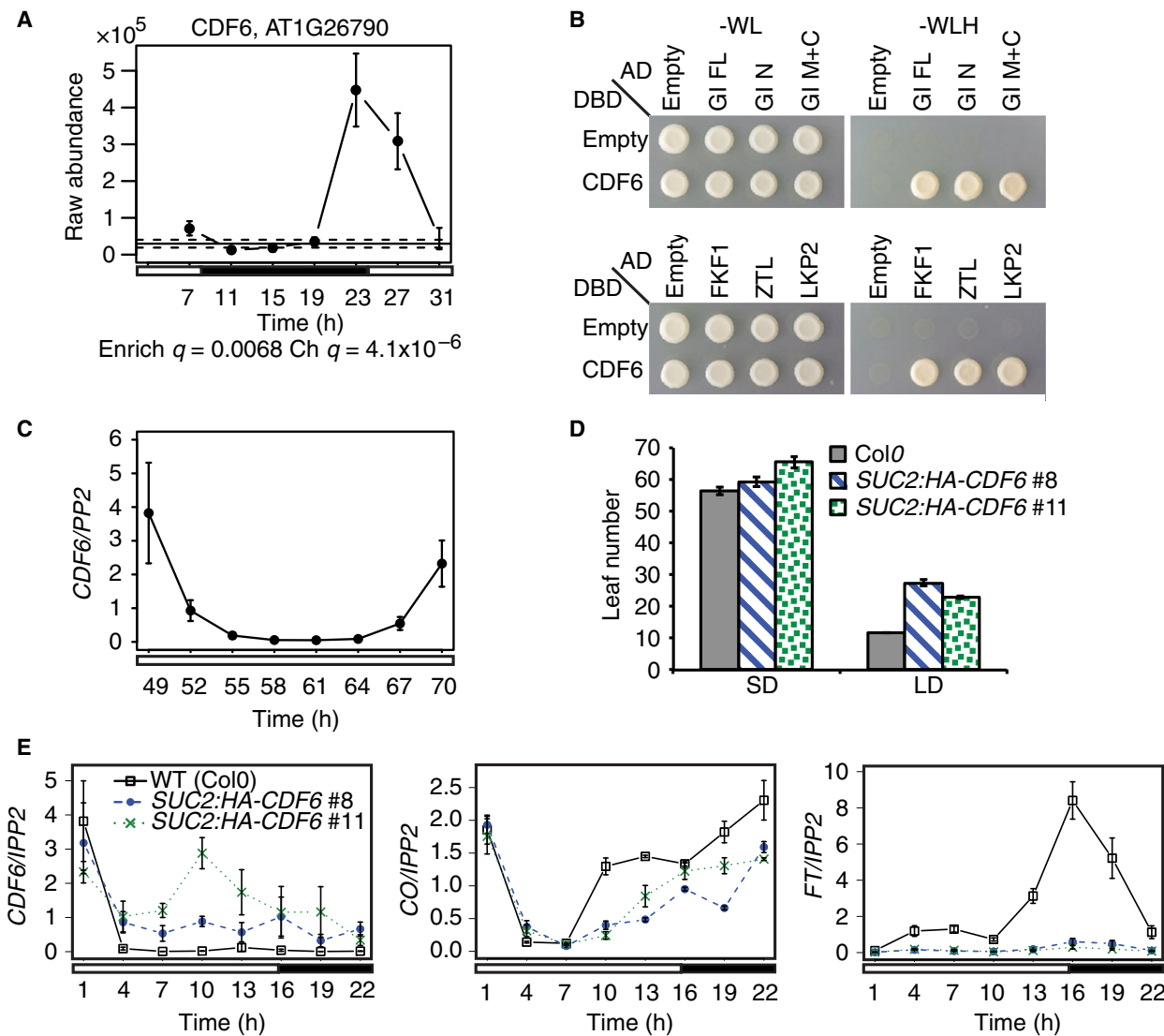


Fig. 4. CDF6 interacts with GI and functions in photoperiodic flowering. (A) GI-interaction profile of CDF6 in the time series study is similar to CDF3 (Fig. 3A). $n = 5$ (except ZT19: $n = 4$) (B) Yeast two-hybrid assays validate interaction of CDF6 with full-length GI, N- and C-terminal domains of GI, as well as ZTL, FKF1 and LKP2. AD, activation domain; DBD, DNA binding domain. (C) Circadian expression profile of *CDF6* mRNA, in WT plants 3 days after transfer to constant light, $n = 3$. (D) *CDF6* over-expression delays flowering of transgenic *SUC2:HA-CDF6* lines more under long days, compared to WT control, than under short days. Each transgenic line differed significantly from WT, *t*-test $P < 0.0001$, except #8 in SD, not significant. $n \geq 16$ (E) mRNA expression profiles of *CDF6*, *CO* and *FT* were tested by qPCR in WT and the overexpressor lines, confirming that *CDF6* suppresses evening *CO* and *FT* expression. $n = 3$.

flowering, where CDF6 protein levels in WT are regulated through interaction with GI and its interacting F-box proteins.

Discussion

Proteostasis, the set of protein-metabolic processes, is expected to be critical for diel rhythms in general, because the removal of transcriptional repressor proteins controls the slow timing of circadian feedback

circuits [8,9]. GI indirectly mediates the degradation of transcriptional repressors through interacting with F-box proteins involved in protein ubiquitination: ZTL mediates targeted degradation of TOC1 [20] and PRR5 [19] with LKP2 and FKF1 contributing [22]. FKF1 targets CDF1 for degradation to regulate photoperiodic flowering, and this FKF1-dependent degradation requires functional GI [31]. GI also has protein chaperone functions to stabilize ZTL and potentially other proteins [45,46]. Our studies identified further

proteostatic proteins associated with GI, and suggested links to metabolic sensing, providing candidates for the unknown targets of GI's proteostatic functions [46] and recalling previous data linking GI, metabolic inputs, and biological timing.

Overexpression of tagged *GI* (*GI-3F6H*) under the 35S promoter in the *gi-2* mutant background rescued the mRNA expression of *CO* and *FT* and flowering time phenotypes of the mutant. GI protein tended to greater abundance during the day than during the night, in line with its light-dependent stabilization by ZTL [23], with an evening peak time similar to native GI protein [27]. The observed immunoprecipitated protein profile closely matched the prediction of a mechanistic clock model that was informed by diverse literature data [5], indicating that the *GI-3F6H* protein conformed to the dynamic, light-responsive behavior expected from previous results (Fig. 3C).

Confirmation of known interactors and the new direct interactor CDF6

The detection of known, indirect interactors of GI such as CUL1/2 among the weakly enriched proteins but not in the qualitative studies validated the time series approach. Among the known, direct interactors of GI that were not detected in our studies, SVP, TEM1, and TEM2 [32], COP1 and ELF3 [29], ELF4 [24], CO [49], and TCP4 [33] are observed or expected to be largely or exclusively nuclear, while SPY [74] and SOS2 [40] are partly nuclear-localized. Analysis of nuclear preparations may be necessary to enrich for these and other, nuclear interactors. Rapid, whole-cell extraction was employed here to facilitate handling the larger sample numbers required to conduct the time series study in quintuplicate [56]. Transcriptional regulators were nevertheless detected, including the known interactor CDF3 [34] and its homolog CDF6 (AT1G26790). Y2H assays validated the interaction of CDF6 with GI N- and C-terminal fragments, as well as with ZTL, FKF1, and LKP2 [35]. Functional overlap with other CDFs was confirmed, as *CDF6* overexpression in leaf phloem companion cells inhibited *CO* and *FT* transcription and delayed flowering in a photoperiod-dependent manner (Fig. 4D, E).

CDF6 transcript expression in long days and constant light peaks around dawn, similar to *CDF1*, *CDF2*, *CDF3*, and *CDF5* [34,35,67]. CDF6 interaction with GI was in antiphase to FKF1 interaction, consistent with CDF6 being largely or specifically degraded *via* this F-box protein. Our qualitative study and others conducted when GI normally accumulates [48] coincide with peak FKF1 abundance, so would not

have detected CDF6 or perhaps CDF3 (Figs 3A and 4A), confirming the utility of the time series approach. However, only 10 proteins (11%) were enriched with a rhythmic profile, so the strong rhythms of FKF1 and the CDFs were uncommon. Rhythmic transcription of GI might normally confer rhythmicity on other partner proteins as it does for ZTL [18,23], in which case we expect mis-expression of GI to alter partner protein accumulation, as *GI-3F6H* does to ZTL. Alternatively, many partner proteins might lack strong rhythmicity.

The large size and proposed proteostasis functions of GI (discussed below) risk false-positive results. GI has not been found localized in or associated with the chloroplast but rather in the nucleus or cytoplasm [15,23,75]. The abundant, plastid-localized proteins enriched as interactors (Data S3 and S4) likely reflect unspecific binding, at least in the case of chloroplast-encoded proteins, which was an expected cost of detecting low-abundance and indirect interactors. Conservatively, we excluded mitochondrial and chloroplast proteins (see Materials and methods; Data S3) from the candidate interactors (Tables 1 and 3). GI might in principle have a physiological role in the metabolism of proteins translated on cytosolic ribosomes, prior to compartmentalization, or of proteins translocated from other compartments to the cytosol for degradation [76].

Metabolic and nuclear functions of GI

Functionally at least, GI links carbon metabolism and timing, *via* a long-term response of the circadian clock to sucrose [39] and the photoperiodic adjustment of the rate of starch biosynthesis [38]. The trehalose-6-phosphate pathway mediates several such sugar responses [77,78]. *TPS8* is a parologue without known enzymatic activity but with diurnally regulated expression, repressed by sucrose [79]. GI interaction with *TPS8* was highly enriched and, unusually, peaked at ZT19 (Fig. 3B), providing one of several possible mechanisms for GI to mediate between metabolism and biological timing.

Few candidate interactors were shared with a previous study using ELF3 and ELF4 bait proteins [48], which each interact with GI [24,29]. For example, RACK1A (AT1G18080) is a promiscuously interacting protein with several reported physiological roles in plants [80]. Its homolog RACK1B (AT1G48630) was also weakly enriched (Table 3). Mammalian RACK1 affects the circadian clock through the interacting core clock transcription factor BMAL1 [81], and contributes to degradation of its parologue hypoxia-

induced factor HIF1a. HIF1a protein regulation is mediated *via* HSP90 and UBP (reviewed in [82]): their *Arabidopsis* homologs were highly enriched in our GI-3F6H datasets.

Potential function of GI in cold response

Some of our candidate interactors may be used to speculate on new mechanisms contributing to GI function. GI enhances cold tolerance independently of CBF signaling [43]. Two of our candidate interactors, REI1-LIKE and GENERAL CONTROL NON-REPRESSIBLE (GCN1; Table 3), have been implicated in cold tolerance through a role in ribosome maturation and regulation of translation initiation, respectively [83,84]. Knowledge of these potential interactors may therefore be helpful to generate hypotheses on how GI mediates cold tolerance.

GI candidate interactors involved in protein metabolism

Protein degradation of clock-relevant, transcriptional repressors was the first biochemical function supported for GI, acting as a scaffold for F-box proteins, though GI's co-chaperone function is now also implicated [18,46]. No further F-box proteins or other ubiquitin E3 ligases were identified here, suggesting that GI mediates further physiological roles through different biochemical mechanisms. Chaperone proteins are typical, nonspecific contaminants of affinity purification studies but direct, physiologically relevant binding of HSP90 with GI has been demonstrated [46]. HSP90 isoform(s) were highly enriched and weakly rhythmic in our time series (Fig. 3B). TPR4, which encodes a tetratricopeptide repeat (TPR) protein with potential to interact with HSP90/HSP70 as a co-chaperone [85] was also strongly enriched (Table 3, Fig. 3B). The HSP70 family proteins that might function with GI and HSP90 [46] were below the significance threshold in the time series study (Table 3) but one (AT5G02500) was the fourth most enriched protein in the qualitative study (Table 1).

In contrast, several other proteins involved in proteostasis were highly and reproducibly enriched. For example, in our time series, two proteasome regulatory proteins were enriched, RPT1A (AT1G53750) and RPN10 (AT4G38630) (Table 3). GI-TAP had identified a different proteasome regulatory protein in rice [86]. TCP-1/cpn60 chaperonin family proteins (AT3G03960; AT3G20050) that can facilitate intercellular trafficking of transcription factors [87] were detected in both the time series and the qualitative studies (Tables 1 and 3).

Interestingly, a GI TAP-MS study in rice identified a potential GI interactor whose closest *Arabidopsis* homologs, ADL3 and ADL6, are also involved in post-Golgi vesicle trafficking [86,88]. Our purification enriched several proteins involved in trans-Golgi or early endosome vesicle trafficking: RAB-A2B and/or RABA3 [89], TUF [90], and HAP13 [91,92]. While we are not aware of any evidence for a Golgi/endosome related function of GI, these candidates may help to generate hypotheses on mechanisms of GI's to date unexplained functions. For example, *Arabidopsis* plants deficient in the Golgi-localized transporter protein PAR1 are more resistant to paraquat due to reduced plastid accumulation of the herbicide [93], and a role of GI in stabilizing such intracellular transport proteins could be an explanation for the increased paraquat resistance of *gi* mutants in addition to the suggested increased resistance to oxidative stress [42].

UBP12 and UBP13 were highly enriched in the time series and were also detected in the preliminary and/or qualitative studies (see note added in proof). Their deubiquitination activity potentially counteracts protein degradation, for example of *Arabidopsis* MYC2 [94], or monoubiquitination, for example of histone H2A [95]. UBP12 and UBP13 are already known to affect the *Arabidopsis* circadian clock, act upstream of *GI* and *CO* in the same photoperiodic flowering time pathway [68], and are recruited to chromatin in association with the histone methylation complex PRC2 [95]. In a final connection, histone de-ubiquitination by USP7, the *Drosophila* homolog of UBP12/UBP13, is allosterically controlled by its interaction with a GMP synthetase [96]. An *Arabidopsis* homolog (AT1G63660) of this enzyme was also enriched in the time series data (Table 3).

Our time series GI TAP-MS results not only identified a new member of CDF proteins functioning in the photoperiodic flowering pathway but also highlighted an extended set of proteostatic functions of GI, with intriguing potential links to metabolic enzymes that are now of interest in other organisms [97]. These provide a novel set of hypotheses on the biochemical mechanisms of flowering regulation and of further physiological effects of GI.

Acknowledgements

We thank Lisa Imrie and Katalin Kis for expert technical support. This work was supported by the Wellcome Trust [096995/Z/11/Z] (to JK), by BBSRC and EPSRC awards [BB/N005147/1] (to KJH) [BB/D019621] (to AJM) and [BB/J009423] (to AJM and TLB), by NIH grants (GM079712 to T.I., NIH/

NIGMS P41 GM103533 to M.J.M.) and by Next-Generation BioGreen 21 Program grant (SSAC, PJ013386, Rural Development Administration, Republic of Korea) to YHS and TI.

Author contributions

Conceptualization, JK, AK, GSG, TI, AJM; Methodology, JK, YHS, RSJ, MJM, TLB; Software, JK, TLB; Formal Analysis, JK, GSG, AK, AZ, RSJ, AJM; Investigation, JK, GSG, AK; Data Curation, JK, TLB.; Writing, JK, GSG, AK, TI, AJM; Visualization, JK., GSG, AK, AJM; Supervision, KJH, TI, AJM; Funding Acquisition, JK, YHS, MJM, KJH, TLB, TI, AJM.

Note added in proof

During preparation of this manuscript, UBP12 and UBP13 were independently identified as interactors of ZTL and LKP2 [98], suggesting that these UBP proteins are indirect interactors of GI.

Data accessibility

Research data pertaining to this article are located at figshare.com: <https://dx.doi.org/10.6084/m9.figshare.741597>

References

- Dodd AN, Kusakina J, Hall A, Gould PD and Hanaoka M (2014) The circadian regulation of photosynthesis. *Photosynth Res* **119**, 181–190.
- Millar AJ (2016) The intracellular dynamics of circadian clocks reach for the light of ecology and evolution. *Annu Rev Plant Biol* **67**, 595–618.
- Flis A, Fernandez AP, Zielinski T, Mengin V, Sulpice R, Stratford K, Hume A, Pokhilko A, Southern MM, Seaton DD et al. (2015) Defining the robust behaviour of the plant clock gene circuit with absolute RNA timeseries and open infrastructure. *Open Biol* **5**, 150042.
- Flis A, Sulpice R, Seaton DD, Ivakov AA, Liput M, Abel C, Millar AJ and Stitt M (2016) Photoperiod-dependent changes in the phase of core clock transcripts and global transcriptional outputs at dawn and dusk in *Arabidopsis*. *Plant, Cell Environ* **39**, 1955–1981.
- Pokhilko A, Fernandez AP, Edwards KD, Southern MM, Halliday KJ and Millar AJ (2012) The clock gene circuit in *Arabidopsis* includes a repressilator with additional feedback loops. *Mol Syst Biol* **8**, 574.
- Fogelmark K and Troein C (2014) Rethinking transcriptional activation in the *Arabidopsis* circadian clock. *PLoS Comput Biol* **10**, e1003705.
- Barneche F, Malapeira J and Mas P (2014) The impact of chromatin dynamics on plant light responses and circadian clock function. *J Exp Bot* **65**, 2895–2913.
- Gerard C, Gonze D and Goldbeter A (2009) Dependence of the period on the rate of protein degradation in minimal models for circadian oscillations. *Philos Trans A Math Phys Eng Sci* **367**, 4665–4683.
- Ruoff P, Loros JJ and Dunlap JC (2005) The relationship between FRQ-protein stability and temperature compensation in the *Neurospora* circadian clock. *Proc Natl Acad Sci* **102**, 17681–17686.
- Pudasaini A, Shim JS, Song YH, Shi H, Kiba T, Somers DE, Imaizumi T and Zoltowski BD (2017) Kinetics of the LOV domain of ZEITLUPE determine its circadian function in *Arabidopsis*. *Elife* **6**, e21646.
- Rédei GP (1962) Supervital mutants of *Arabidopsis*. *Genetics* **47**, 443–460.
- Koornneef M, Hanhart CJ and van der Veen JH (1991) A genetic and physiological analysis of late flowering mutants in *Arabidopsis thaliana*. *Mol Gen Genet* **229**, 57–66.
- Park DH, Somers DE, Kim YS, Choy YH, Lim HK, Soh MS, Kim HJ, Kay SA and Nam HG (1999) Control of circadian rhythms and photoperiodic flowering by the *Arabidopsis GIGANTEA* gene. *Science* **285**, 1579–1582.
- Fowler S, Lee K, Onouchi H, Samach A, Richardson K, Coupland G and Putterill J (1999) *GIGANTEA*: a circadian clock-controlled gene that regulates photoperiodic flowering in *Arabidopsis* and encodes a protein with several possible membrane-spanning domains. *EMBO J* **18**, 4679–4688.
- Mizoguchi T, Wright L, Fujiwara S, Cremer F, Lee K, Onouchi H, Mouradov A, Kamada H, Putterill J and Coupland G (2005) Distinct roles of *GIGANTEA* in promoting flowering and regulating circadian rhythms in *Arabidopsis*. *Plant Cell* **17**, 2255–2270.
- Kevei É, Gyula P, Hall A, Kozma-Bognár L, Kim W-Y, Eriksson ME, Tóth R, Hanano S, Fehér B, Southern MM et al. (2006) Forward genetic analysis of the circadian clock separates the multiple functions of ZEITLUPE. *Plant Physiol* **140**, 933–945.
- Martin-Tryon EL, Kreps JA and Harmer SL (2007) *GIGANTEA* acts in blue light signaling and has biochemically separable roles in circadian clock and flowering time regulation. *Plant Physiol* **143**, 473–486.
- Kim W-Y, Fujiwara S, Suh S-S, Kim J, Kim Y, Han L, David K, Putterill J, Nam HG and Somers DE (2007) ZEITLUPE is a circadian photoreceptor stabilized by GIGANTEA in blue light. *Nature* **449**, 356–360.
- Kiba T, Henriques R, Sakakibara H and Chua NH (2007) Targeted degradation of PSEUDO-RESPONSE REGULATOR5 by an SCF^{ZTL} complex regulates clock

function and photomorphogenesis in *Arabidopsis thaliana*. *Plant Cell* **19**, 2516–2530.

20 Mas P, Kim WY, Somers DE and Kay SA (2003) Targeted degradation of TOC1 by ZTL modulates circadian function in *Arabidopsis thaliana*. *Nature* **426**, 567–570.

21 Han L, Mason M, Risseeuw EP, Crosby WL and Somers DE (2004) Formation of an SCF^{ZTL} complex is required for proper regulation of circadian timing. *Plant J* **40**, 291–301.

22 Baudry A, Ito S, Song YH, Strait AA, Kiba T, Lu S, Henriques R, Pruneda-Paz JL, Chua N-H, Tobin EM *et al.* (2010) F-box proteins FKF1 and LKP2 act in concert with ZEITLUPE to control *Arabidopsis* clock progression. *Plant Cell* **22**, 606–622.

23 Kim J, Geng R, Gallenstein RA and Somers DE (2013) The F-box protein ZEITLUPE controls stability and nucleocytoplasmic partitioning of GIGANTEA. *Development* **140**, 4060–4069.

24 Kim Y, Lim J, Yeom M, Kim H, Kim J, Wang L, Kim WY, Somers DE and Nam HG (2013) ELF4 regulates GIGANTEA chromatin access through subnuclear sequestration. *Cell Rep* **3**, 671–677.

25 Kim Y, Han S, Yeom M, Kim H, Lim J, Cha J-Y, Kim W-Y, Somers DE, Putterill J, Nam HG *et al.* (2013) Balanced nucleocytosolic partitioning defines a spatial network to coordinate circadian physiology in plants. *Dev Cell* **26**, 73–85.

26 Dixon LE, Knox K, Kozma-Bognar L, Southern MM, Pokhilko A and Millar AJ (2011) Temporal repression of core circadian genes is mediated through EARLY FLOWERING 3 in *Arabidopsis*. *Curr Biol* **21**, 120–125.

27 David KM, Armbruster U, Tama N and Putterill J (2006) Arabidopsis GIGANTEA protein is post-transcriptionally regulated by light and dark. *FEBS Lett* **580**, 1193–1197.

28 Nusinow D, Helfer A, Hamilton EE, King JJ, Imaizumi T, Schultz TF, Farré EM and Kay SA (2011) The ELF4-ELF3-LUX complex links the circadian clock to diurnal control of hypocotyl growth. *Nature* **475**, 398–402.

29 Yu JW, Rubio V, Lee NY, Bai S, Lee SY, Kim SS, Liu L, Zhang Y, Irigoyen ML, Sullivan JA *et al.* (2008) COP1 and ELF3 control circadian function and photoperiodic flowering by regulating GI stability. *Mol Cell* **32**, 617–630.

30 Samach A, Onouchi H, Gold SE, Ditta GS, Schwarz-Sommer Z, Yanofsky MF and Coupland G (2000) Distinct roles of CONSTANS target genes in reproductive development of *Arabidopsis*. *Science* **288**, 1613–1616.

31 Sawa M, Nusinow DA, Kay SA and Imaizumi T (2007) FKF1 and GIGANTEA complex formation is required for day-length measurement in *Arabidopsis*. *Science* **318**, 261–265.

32 Sawa M and Kay SA (2011) GIGANTEA directly activates *Flowering Locus T* in *Arabidopsis thaliana*. *Proc Natl Acad Sci USA* **108**, 11698–11703.

33 Kubota A, Ito S, Shim JS, Johnson RS, Song YH, Breton G, Goralogia GS, Kwon MS, Laboy Cintron D, Koyama T *et al.* (2017) TCP4-dependent induction of CONSTANS transcription requires GIGANTEA in photoperiodic flowering in *Arabidopsis*. *PLoS Genet* **13**, e1006856.

34 Imaizumi T, Schultz TF, Harmon FG, Ho LA and Kay SA (2005) FKF1 F-box protein mediates cyclic degradation of a repressor of CONSTANS in *Arabidopsis*. *Science* **309**, 293–297.

35 Fornara F, Panigrahi KC, Gissot L, Sauerbrunn N, Ruhl M, Jarillo JA and Coupland G (2009) *Arabidopsis* DOF transcription factors act redundantly to reduce CONSTANS expression and are essential for a photoperiodic flowering response. *Dev Cell* **17**, 75–86.

36 Song YH, Smith RW, To BJ, Millar AJ and Imaizumi T (2012) FKF1 conveys timing information for CONSTANS stabilization in photoperiodic flowering. *Science* **336**, 1045–1049.

37 Eimert K, Wang SM, Lue WI and Chen J (1995) Monogenic recessive mutations causing both late floral initiation and excess starch accumulation in *Arabidopsis*. *Plant Cell* **7**, 1703–1712.

38 Mugford ST, Fernandez O, Brinton J, Flis A, Krohn N, Encke B, Feil R, Sulpice R, Lunn JE, Stitt M *et al.* (2014) Regulatory properties of ADP glucose pyrophosphorylase are required for adjustment of leaf starch synthesis in different photoperiods. *Plant Physiol* **166**, 1733–1747.

39 Dalchau N, Baek SJ, Briggs HM, Robertson FC, Dodd AN, Gardner MJ, Stancombe MA, Haydon MJ, Stan G-B, Gonçalves JM *et al.* (2011) The circadian oscillator gene GIGANTEA mediates a long-term response of the *Arabidopsis thaliana* circadian clock to sucrose. *Proc Natl Acad Sci* **108**, 5104–5109.

40 Kim W-Y, Ali Z, Park HJ, Park SJ, Cha J-Y, Perez-Hormaeche J, Quintero FJ, Shin G, Kim MR, Qiang Z *et al.* (2013) Release of SOS2 kinase from sequestration with GIGANTEA determines salt tolerance in *Arabidopsis*. *Nat Commun* **4**, 1352.

41 Riboni M, Galbiati M, Tonelli C and Conti L (2013) GIGANTEA enables drought escape response via abscisic acid-dependent activation of the florigens and SUPPRESSOR OF OVEREXPRESSION OF CONSTANS. *Plant Physiol* **162**, 1706–1719.

42 Kurepa J, Smalle J, Van Montagu M and Inzé D (1998) Oxidative stress tolerance and longevity in *Arabidopsis*: the late-flowering mutant *gigantea* is tolerant to paraquat. *Plant J* **14**, 759–764.

43 Cao S, Ye M and Jiang S (2005) Involvement of GIGANTEA gene in the regulation of the cold stress response in *Arabidopsis*. *Plant Cell Rep* **24**, 683–690.

44 Fornara F, De Montaigu A, Sánchez-Villarreal A, Takahashi Y, Van Themaat EVL, Huettel B, Davis SJ and Coupland G (2015) The GI-CDF module of *Arabidopsis* affects freezing tolerance and growth as well as flowering. *Plant J* **81**/**5**, 695–706.

45 Kim T-S, Kim W-Y, Fujiwara S, Kim J, Cha J-Y, Park JH, Lee SY and Somers DE (2011) HSP90 functions in the circadian clock through stabilization of the client F-box protein ZEITLUPE. *Proc Natl Acad Sci* **108**, 16843–16848.

46 Cha JY, Kim J, Kim TS, Zeng Q, Wang L, Lee SY, Kim WY and Somers DE (2017) GIGANTEA is a co-chaperone which facilitates maturation of ZEITLUPE in the *Arabidopsis* circadian clock. *Nat Commun* **8**, 3.

47 Imaizumi T and Kay SA (2006) Photoperiodic control of flowering: not only by coincidence. *Trends Plant Sci* **11**, 550–558.

48 Huang H, Alvarez S, Bindbeutel R, Shen Z, Naldrett MJ, Evans BS, Briggs SP, Hicks LM, Kay SA and Nusinow DA (2016) Identification of evening complex associated proteins in *Arabidopsis* by affinity purification and mass spectrometry. *Mol Cell Proteomics* **15**, 201–217.

49 Song YH, Estrada DA, Johnson RS, Kim SK, Lee SY, MacCoss MJ and Imaizumi T (2014) Distinct roles of FKF1, GIGANTEA, and ZEITLUPE proteins in the regulation of CONSTANS stability in *Arabidopsis* photoperiodic flowering. *Proc Natl Acad Sci* **111**, 17672–17677.

50 Nakagawa T, Nakamura S, Tanaka K, Kawamukai M, Suzuki T, Nakamura K, Kimura T and Ishiguro S (2008) Development of R4 gateway binary vectors (R4pGWB) enabling high-throughput promoter swapping for plant research. *Biosci Biotechnol Biochem* **72**, 624–629.

51 Eng JK, Jahan TA and Hoopmann MR (2013) Comet: an open-source MS/MS sequence database search tool. *Proteomics* **13**, 22–24.

52 Vizcaino JA, Csordas A, del-Toro N, Dianes JA, Griss J, Lavidas I, Mayer G, Perez-Riverol Y, Reisinger F, Ternent T *et al.* (2016) 2016 update of the PRIDE database and its related tools. *Nucleic Acids Res* **44**, D447–D456.

53 Hughes ME, Hogenesch JB and Kornacker K (2010) JTK_CYCLE: an efficient nonparametric algorithm for detecting rhythmic components in genome-scale data sets. *J Biol Rhythms* **25**, 372–380.

54 Suzuki R and Shimodaira H (2015) pvcust: hierarchical clustering with P-values via multiscale bootstrap resampling. *Bioinformatics* **22**/**12**, 1540–1542.

55 Alexa A and Rahnenführer J (2010) Enrichment analysis for Gene Ontology. R Packag. version 2.16.0.

56 Alexa A, Rahnenführer J and Lengauer T (2006) Improved scoring of functional groups from gene expression data by decorrelating GO graph structure. *Bioinformatics* **22**, 1600–1607.

57 Krahmer J, Hindle MM, Martin SF, Le Bihan T and Millar AJ (2015) Sample preparation for phosphoproteomic analysis of circadian time series in *Arabidopsis thaliana*. *Methods Enzymol* **551**, 405–431.

58 Hooper CM, Castleden IR, Tanz SK, Aryamanesh N and Millar AH (2017) SUBA4: the interactive data analysis centre for *Arabidopsis* subcellular protein locations. *Nucl Acids Res* **45**, D1064–D1074.

59 Chatr-aryamontri A, Oughtred R, Boucher L, Rust J, Chang C, Kolas NK, O'Donnell L, Oster S, Theesfeld C, Sellam A *et al.* (2017) The BioGRID interaction database: 2017 update. *Nucl Acids Res* **45**, D369–D379.

60 Nakayama M, Kikuno R and Ohara O (2002) Protein-protein interactions between large proteins: two-hybrid screening using a functionally classified library composed of long cDNAs. *Genome Res* **12**, 1773–1784.

61 Hoops S, Sahle S, Gauges R, Lee C, Pahle J, Simus N, Singhal M, Xu L, Mendes P and Kummer U (2006) COPASI—a COmplex PAthway SImulator. *Bioinformatics* **22**, 3067–3074.

62 Chew YH, Seaton DD, Mengin V, Flis A, Mugford ST, Smith AM, Stitt M and Millar AJ (2017) Linking circadian time to growth rate quantitatively via carbon metabolism. *bioRxiv*, Article no: 105437.

63 Thomas PD, Campbell MJ, Kejariwal A, Mi H and Karlak B (2003) PANTHER: a library of protein families and subfamilies indexed by function. *Genome Res* **13**, 2129–2141.

64 Takahashi N, Kuroda H, Kuromori T, Hirayama T, Seki M, Shinozaki K, Shimada H and Matsui M (2004) Expression and interaction analysis of *Arabidopsis Skp1*-related genes. *Plant Cell Physiol* **45**, 83–91.

65 Nelson DC, Lasswell J, Rogg LE, Cohen MA and Bartel B (2000) FKF1, a clock-controlled gene that regulates the transition to flowering in *Arabidopsis*. *Cell* **101**, 331–340.

66 Somers DE, Schultz TF, Milnamow M and Kay SA (2000) ZEITLUPE encodes a novel clock-associated PAS protein from *Arabidopsis*. *Cell* **101**, 319–329.

67 Seaton DD, Smith RW, Song YH, MacGregor DR, Stewart K, Steel G, Foreman J, Penfield S, Imaizumi T, Millar AJ *et al.* (2015) Linked circadian outputs control elongation growth and flowering in response to photoperiod and temperature. *Mol Syst Biol* **11**, 776.

68 Mockler T, Michael T, Priest H, Shen R, Sullivan C, Givan S, McEntee C, Kay S and Chory J (2007) THE DIURNAL PROJECT: diurnal and circadian expression profiling, model-based pattern matching and promoter analysis. *Cold Spring Harb Symp Quant Biol* **72**, 353–363.

69 Imaizumi T, Tran HG, Swartz TE, Briggs WR and Kay SA (2003) FKF1 is essential for photoperiodic-specific light signalling in *Arabidopsis*. *Nature* **426**, 302–306.

70 Cui X, Lu F, Li Y, Xue Y, Kang Y, Zhang S, Qiu Q, Cui X, Zheng S, Liu B *et al.* (2013) Ubiquitin-specific

proteases UBP12 and UBP13 act in circadian clock and photoperiodic flowering regulation in *Arabidopsis*. *Plant Physiol* **162**, 897–906.

71 Goralagia GS, Liu T-K, Zhao L, Panipinto PM, Groover ED, Bains YS and Imaizumi T (2017) CYCLING DOF FACTOR 1 represses transcription through the TOPLESS co-repressor to control photoperiodic flowering in *Arabidopsis*. *Plant J* **92**, 244–262.

72 An H, Roussel C, Suárez-López P, Corbesier L, Vincent C, Piñeiro M, Hepworth S, Mouradov A, Justin S, Turnbull C *et al.* (2004) CONSTANS acts in the phloem to regulate a systemic signal that induces photoperiodic flowering of *Arabidopsis*. *Development* **131**, 3615–3626.

73 Takada S and Goto K (2003) TERMINAL FLOWER2, an *Arabidopsis* homolog of HETEROCHROMATIN PROTEIN1, counteracts the activation of *FLOWERING LOCUS T* by CONSTANS in the vascular tissues of leaves to regulate flowering time. *Plant Cell* **15**, 2856–2865.

74 Tseng T-S, Salomé PA, McClung CR and Olszewski NE (2004) SPINDLY and GIGANTEA interact and act in *Arabidopsis thaliana* pathways involved in light responses, flowering, and rhythms in cotyledon movements. *Plant Cell* **16**, 1550–1563.

75 Huq E, Tepperman JM and Quail PH (2000) GIGANTEA is a nuclear protein involved in phytochrome signaling in *Arabidopsis*. *Proc Natl Acad Sci* **97**, 9789–9794.

76 Svozil J, Hirsch-Hoffmann M, Dudler R, Gruissem W and Baerenfaller K (2014) Protein abundance changes and ubiquitylation targets identified after inhibition of the proteasome with syringolin A. *Mol Cell Proteomics* **13**, 1523–1536.

77 Ramon M, De Smet I, Vandesteene L, Naudts M, Leyman B, Van Dijck P, Rolland F, Beeckman T and Thevelein JM (2009) Extensive expression regulation and lack of heterologous enzymatic activity of the Class II trehalose metabolism proteins from *Arabidopsis thaliana*. *Plant, Cell Environ* **32**, 1015–1032.

78 Wahl V, Ponnu J, Schlereth A, Arrivault S, Langenecker T, Franke A, Feil R, Lunn JE, Stitt M and Schmid M (2013) Regulation of flowering by trehalose-6-phosphate signaling in *Arabidopsis thaliana*. *Science* **339**, 704–707.

79 Usadel B, Bläsing OE, Gibon Y, Retzlaff K, Höhne M, Günther M and Stitt M (2008) Global transcript levels respond to small changes of the carbon status during progressive exhaustion of carbohydrates in *Arabidopsis* rosettes. *Plant Physiol* **146**, 1834–1861.

80 Islas-Flores T, Rahman A, Ullah H and Villanueva MA (2015) The receptor for activated C kinase in plant signaling: tale of a promiscuous little molecule. *Front Plant Sci* **6**, 1090.

81 Robles P, Fleury D, Candela H, Cnops G, Alonso-Peral MM, Anami S, Falcone A, Caldana C, Willmitzer L, Ponce MR *et al.* (2010) The *RON1/FRY1/SAL1* gene is required for leaf morphogenesis and venation patterning in *Arabidopsis*. *Plant Physiol* **152**, 1357–1372.

82 Wilkins SE, Abboud MI, Hancock RL and Schofield CJ (2016) Targeting protein-protein interactions in the HIF system. *ChemMedChem* **11**, 773–786.

83 Schmidt S, Dethloff F, Beine-Golovchuk O and Kopka J (2013) The REIL1 and REIL2 proteins of *Arabidopsis thaliana* are required for leaf growth in the cold. *Plant Physiol* **163**, 1623–1639.

84 Wang L, Li H, Zhao C, Li S, Kong L, Wu W, Kong W, Liu Y, Wei Y, Zhu JK *et al.* (2017) The inhibition of protein translation mediated by AtGCN1 is essential for cold tolerance in *Arabidopsis thaliana*. *Plant, Cell Environ* **40**, 56–68.

85 Prasad BD, Goel S and Krishna P (2010) *In silico* identification of carboxylate clamp type tetratricopeptide repeat proteins in *Arabidopsis* and rice as putative co-chaperones of Hsp90/Hsp70. *PLoS ONE* **5**, e12761.

86 Abe M, Fujiwara M, Kurotani KI, Yokoi S and Shimamoto K (2008) Identification of dynamin as an interactor of rice GIGANTEA by tandem affinity purification (TAP). *Plant Cell Physiol* **49**, 420–432.

87 Xu XM, Wang J, Xuan Z, Goldshmidt A, Borrill PGM, Hariharan N, Kim JY and Jackson D (2011) Chaperonins facilitate KNOTTED1 cell-to-cell trafficking and stem cell function. *Science* **333**, 1141–1144.

88 Huang J, Fujimoto M, Fujiwara M, Fukao Y, Arimura SI and Tsutsumi N (2015) *Arabidopsis* dynamin-related proteins, DRP2A and DRP2B, function coordinately in post-Golgi trafficking. *Biochem Biophys Res Commun* **456**, 238–244.

89 Chow C-M, Neto H, Foucart C and Moore I (2008) Rab-A2 and Rab-A3 GTPases define a *trans*-Golgi endosomal membrane domain in *Arabidopsis* that contributes substantially to the cell plate. *Plant Cell* **20**, 101–123.

90 Strompen G, Dettmer J, Stierhof YD, Schumacher K, Jürgens G and Mayer U (2005) *Arabidopsis* vacuolar H⁺-ATPase subunit E isoform 1 is required for Golgi organization and vacuole function in embryogenesis. *Plant J* **41**, 125–132.

91 Wang J-G, Li S, Zhao X-Y, Zhou L-Z, Huang G-Q, Feng C and Zhang Y (2013) HAPLESS13, the *Arabidopsis* 1 Adapton, is essential for protein sorting at the trans-golgi network/early endosome. *Plant Physiol* **162**, 1897–1910.

92 Park M, Song K, Reichardt I, Kim H, Mayer U, Stierhof Y-D, Hwang I and Jürgens G (2013) *Arabidopsis* μ-adaptin subunit AP1M of adaptor

protein complex 1 mediates late secretory and vacuolar traffic and is required for growth. *Proc Natl Acad Sci* **110**, 10318–10323.

93 Li J, Mu J, Bai J, Fu F, Zou T, An F, Zhang J, Jing H, Wang Q, Li Z *et al.* (2013) PARAQUAT RESISTANT1, a golgi-localized putative transporter protein, is involved in intracellular transport of paraquat. *Plant Physiol* **162**, 470–483.

94 Jeong JS, Jung C, Seo JS, Kim JK and Chua NH (2017) The deubiquitinating enzymes UBP12 and UBP13 positively regulate MYC2 levels in jasmonate responses. *Plant Cell* **29**, 1406–1424.

95 Derkacheva M, Liu S, Figueiredo DD, Gentry M, Mozgova I, Nanni P, Tang M, Mannervik M, Kohler C and Hennig L (2016) H2A deubiquitinases UBP12/13 are part of the *Arabidopsis* polycomb group protein system. *Nat Plants* **2**, 16126.

96 van der Knaap JA, Kumar BR, Moshkin YM, Langenberg K, Krijgsveld J, Heck AJ, Karch F and Verrijzer CP (2005) GMP synthetase stimulates histone H2B deubiquitylation by the epigenetic silencer USP7. *Mol Cell* **17**, 695–707.

97 van der Knaap JA and Verrijzer CP (2016) Undercover: gene control by metabolites and metabolic enzymes. *Genes Dev* **30**, 2345–2369.

98 Lee C-M, Feke A, Li M-W, Adamchek C, Webb K, Pruneda-Paz J, Bennett EJ, Kay SA and Gendron JM (2018) Decoys Untangle Complicated Redundancy and Reveal Targets of Circadian Clock F-Box Proteins. *Plant Physiol* **177**, 1170–1186.

Supporting information

Additional supporting information may be found online in the Supporting Information section at the end of the article.

Fig. S1. Validation of the GI-TAP procedure.

Fig. S2. Outlier analysis of the GI-TAP time series study.

Fig. S3. Transcript expression profiles of *GI* (A), *FKF1* (B), *ZTL* (C), and *FKF1* (D) from the diurnal website (<http://diurnal.mocklerlab.org>, [94]), using the ‘short-days’ condition.

Table S1. Primer sequences.

Data S1. List of proteins identified by LC-MS analysis of bands excised from silver-stained gel after GI-TAP (Preliminary study, Fig. 1F), includes original Mascot search output files.

Data S2. List of proteins identified in the qualitative, on-bead digest analysis (Qualitative study, Fig. 1F), with peptide counts for GI-3F6H samples and WT background controls.

Data S3. Proteins identified in the time series study (Fig. 1F), with quantitation and statistics, put together from output generated by scripts in Data S7, and Data S8.

Data S4. GO analysis on time series study: TopGO analysis results of GI-3F6H time series.

Data S5. PCA on time series: R script, input files, output files; all on raw abundance data.

Data S6. Gene ontology analysis on time series study, for Data S4.

Data S7. Progenesis protein data export files, and analysis with R script for statistics on time series study (for Data S3 and Table 3).

Data S8. JTK_CYCLE analysis of time series study.

Data S9. Progenesis peptide measurements output file for time series study.